Edelweiss Applied Science and Technology
ISSN: 2576-8484
Vol. 10, No. 2, 276-296
2026
Publisher: Learning Gate
DOI: 10.55214/2576-8484.v10i2.12036

Structural optimization of an external gear pump casing and gears using finite element analysis and response surface methodology

N. Habi[1], M. Bachene[1], R. Rebhi[2], A. Abdellah El-Hadj[1], Mohammed R. Hayal[3], Sk. Hasane Ahammad[4], Ebrahim E. Elsayed[5], Davron Aslonqulovich Juraev[6,7,8*]
[1]Laboratory of Mechanics, Physics and Mathematical Modelling (LMP2M), University of Medea, Algeria.
[2]Laboratory of Renewable Energies and Materials-LERM, University of Medea, Algeria.
[3]Department of Electronics and Communications Engineering, Faculty of Engineering, Mansoura University, Mansoura, Egypt; mohammedraisan@gmail.com (M.R.H.).
[4]Department of Electronics and Communication Engineering, Koneru Lakshmaiah Education Foundation (KLEF), Andhra Pradesh, India; ahammadklu@gmail.com (S.H.A.).
[5]Department of Electronics and Communications Engineering, Faculty of Engineering, Mansoura University, Mansoura 35516, Egypt; engebrahem16@std.mans.edu.eg; ebrahimeldesoky@gmail.com (E.E.E.).
[6]Scientific Research Centre, Baku Engineering University, Baku AZ0102, Azerbaijan; djuraev@beu.edu.az (D.A.J.).
[7]Scientific Department, University of Economics and Pedagogy, Karshi 180100, Uzbekistan.
[8]Department of Mathematical Analysis and Differential Equations, Karshi State University, Karshi 180119, Uzbekistan.

Abstract: This study presents the structural analysis and optimization of an external hydraulic gear pump with the aim of improving mechanical performance while reducing material usage and overall mass. The work addresses two main aspects: optimization of the pump casing and optimization of the internal gears. The geometric model was constructed in SolidWorks with fully parameterized dimensions to enable an efficient optimization workflow. Finite Element Analysis (FEA) in ANSYS Workbench was used to evaluate stress and deformation under realistic operating conditions. For the pump casing, simulation results were integrated into a Response Surface Methodology (RSM) framework to assess the influence of geometric parameters on structural behavior. The optimized casing achieved a 9.5% weight reduction while ensuring structural integrity, with a maximum deformation of 0.031 mm, a maximum stress of 127 MPa, and a safety factor of 3. The efficiency-to-mass ratio improved from 7.9 to 8.8. In parallel, optimization of the gear pair focused on minimizing stress concentrations and improving stiffness. Using ANSYS simulations combined with RSM, the optimized gear design reduced von Mises stress from 239.4 MPa to 224 MPa, reflecting better load distribution and enhanced durability. Overall, the results demonstrate the effectiveness of integrating finite element simulation with response surface optimization to achieve structural and performance improvements in hydraulic gear pumps.

Keywords: *Efficiency to mass ratio, External gear pump casing, Finite element analysis, Gears, Optimization, Response surface methodology.*

1. Introduction

Fluid transport systems play a vital role in many industrial applications. Various sectors, such as oil and gas, chemical industries, and hydraulic systems, rely on them to ensure efficient and consistent fluid flow [1]. Pumping technologies are a key component of these systems, directly impacting performance and sustainability. Among the commonly used pumping technologies, gear pumps stand out as an effective solution for transferring fluids in controlled quantities and at constant pressure. These pumps are characterized by their simple construction and high efficiency, making them ideal for applications that require consistent and precise flow, such as lubrication and hydraulic systems, and various industrial equipment [2].

History: Received: 26 November 2025; Revised: 13 January 2026; Accepted: 16 January 2026; Published: 6 February 2026
* Correspondence: djuraev@beu.edu.az juraevdavron12@gmail.com

External gear pumps, a category of positive displacement pumps, are frequently used for transferring water, light oils, chemical additives, resins, or solvents. They are especially favored in scenarios requiring precise dosing or high-pressure delivery and are widely employed in hydraulic circuits and fluid power systems for energy transfer [3].

Researchers have increasingly relied on numerical simulations to explore methods for minimizing pressure and flow fluctuations in gear pumps [4]. Given the critical role these pumps play in industrial applications and their proven reliability [5], boosting overall efficiency [6], minimizing pressure pulsations [7], continuous efforts are being made to enhance their performance. These advancements span several key aspects, including raising the maximum operating pressures and reducing the overall weight of pump systems [8]. Such improvements significantly contribute to making gear pumps more effective and adaptable in various industrial environments.

Finite Element Analysis (FEA) has become a fundamental tool for evaluating the structural performance of mechanical components, allowing engineers to predict stress distribution, deformation, and failure points before manufacturing [9, 10]. Structural analysis using ANSYS software enables detailed insights into stress and deformation behaviors under operational conditions, facilitating design improvements [11, 12]. In the context of external gear pumps, recent studies have demonstrated that lightweight designs achieved through optimization techniques can significantly enhance pump efficiency while maintaining durability [8, 13].

Response Surface Methodology (RSM) is a powerful statistical tool for optimization, especially in engineering, where multiple variables influence performance. Applying RSM to mechanical structures allows researchers to systematically explore design modifications to achieve optimal results without compromising mechanical integrity [14, 15]. Previous studies have successfully integrated FEA and RSM to optimize gear pumps, demonstrating improvements in weight reduction, stress distribution, hydrodynamics, and energy efficiency [16, 17].

Additional investigations into external gear pump optimization have emerged, focusing on performance, material selection, and structural enhancement. Yoon et al. [18] conducted detailed 3D numerical simulations to evaluate the effects of geometric parameters such as gear tip and lateral clearances on flow rate, pressure peaks, and cavitation, revealing their crucial role in pump efficiency. Ivanov et al. [19] introduced the use of hypocycloid and epicycloid tooth profiles, demonstrating notable performance gains while maintaining structural strength. Material-based structural analysis was performed by Kattimani et al. [20], who compared aluminum and cast-iron gear pumps using ANSYS, highlighting improvements in functionality and efficiency through design optimization.

Innovative gear geometry strategies were explored by Gulati et al. [21], where asymmetric involute gears were optimized using a multi-objective approach to minimize flow irregularities and reduce pump size. The deformation behavior under pressure-induced loadings was also investigated by Cieślicki and Karpenko [22], emphasizing how increased internal clearances negatively affect volumetric efficiency. Stress distribution studies by Kollek et al. [23] on micro-gear pumps revealed that shifting liners by 2.2 mm improved structural integrity and durability.

Further structural assessments by Cieślicki et al. [24] involved developing and validating a finite element model to evaluate strain, stress, and displacement under real operational conditions. Similarly, Guo [25] compared the performance of QT450-10 and ZL111 materials for gear pump bodies to ensure mechanical reliability. Ghionea [26] focused on the parametric modeling and optimization of a catalytic gear pump across extended flow rate ranges, while Rodionov et al. [27] addressed challenges in micropump design, including gear geometry and plastic material applications. Lastly, Zharkevich et al. [28] investigated weight reduction through material optimization and finite element simulations under 28 MPa pressure, achieving reduced stress concentrations without compromising strength.

Recent contributions by Ozsoy and Kurnaz [29] focused on the structural optimization of a hydraulic gear pump cover using Design of Experiments (DOE) and Response Surface Methodology (RSM), which involved reducing the wall thickness of the component, followed by experimental validation to confirm the accuracy of simulation outcomes. Additional studies by Kollek and Radziwanowska [30] explored the

Edelweiss Applied Science and Technology
ISSN: 2576-8484
Vol. 10, No. 2: 276-296, 2026
DOI: 10.55214/2576-8484.v10i2.12036

optimization of a micro-gear pump casing, aiming to minimize both structural mass and overall dimensions. Using ANSYS software, they demonstrated that design modifications with up to 25% volume reduction could retain essential strength and stiffness requirements. Similarly, Kollek and Radziwanowska [31] conducted a static analysis to enhance the mass efficiency of a micro-gear pump body. The optimized design resulted in a 25% weight reduction and improved energy efficiency by over 30% compared to the original configuration.

This study presents a comprehensive structural optimization analysis of an external hydraulic gear pump, addressing both the casing and the internal gear pair to enhance mechanical performance while reducing weight and material usage. Using ANSYS simulations in combination with response surface methodology (RSM), the optimized gear design achieved a significant reduction in von Mises stress from 192.78 MPa to 152.91 MPa, indicating improved load distribution and stiffness. The pump casing was parametrically modeled in SolidWorks to ensure precise geometric control, followed by finite element analysis (FEA) in ANSYS to evaluate stress distribution and deformation under operational pressures. In contrast to previous work by Kollek and Radziwanowska [31], which applied dimensionality reduction in ANSYS without advanced optimization, the present study systematically integrates RSM for both the casing and gear components. Collectively, these improvements are expected to reduce wear, minimize mechanical losses, and increase the long-term reliability of the hydraulic gear pump, demonstrating the effectiveness of combining finite element simulation with RSM-based optimization for structural enhancement in hydraulic machinery.

2. External Gear Pump

The gear pump is a fundamental component in fluid transfer systems, known for its efficiency and reliability in maintaining a consistent flow rate across various industrial applications. Its design includes several key components, each playing a vital role in the pump's overall performance. These components include the casing, driving and driven gears, shafts, suction and discharge ports, sealing systems, anti-extrusion rings, and balance plates. The casing serves as the main structure that encloses and protects the internal parts. It is typically made from lightweight and durable materials such as aluminum, which helps reduce weight, simplify installation, and provide corrosion resistance. The precisely manufactured driving and driven gears work together to ensure consistent fluid flow while minimizing leakage and maintaining volumetric efficiency. Sealing systems prevent fluid leakage and ensure pressure integrity within the system. Anti-extrusion rings protect the sealing elements, enabling smooth pump operation without compromising efficiency. Figure 1 shows a detailed view of the external gear pump design, while Table 1 presents the specifications of the pump used in our study.

Edelweiss Applied Science and Technology
ISSN: 2576-8484
Vol. 10, No. 2: 276-296, 2026
DOI: 10.55214/2576-8484.v10i2.12036

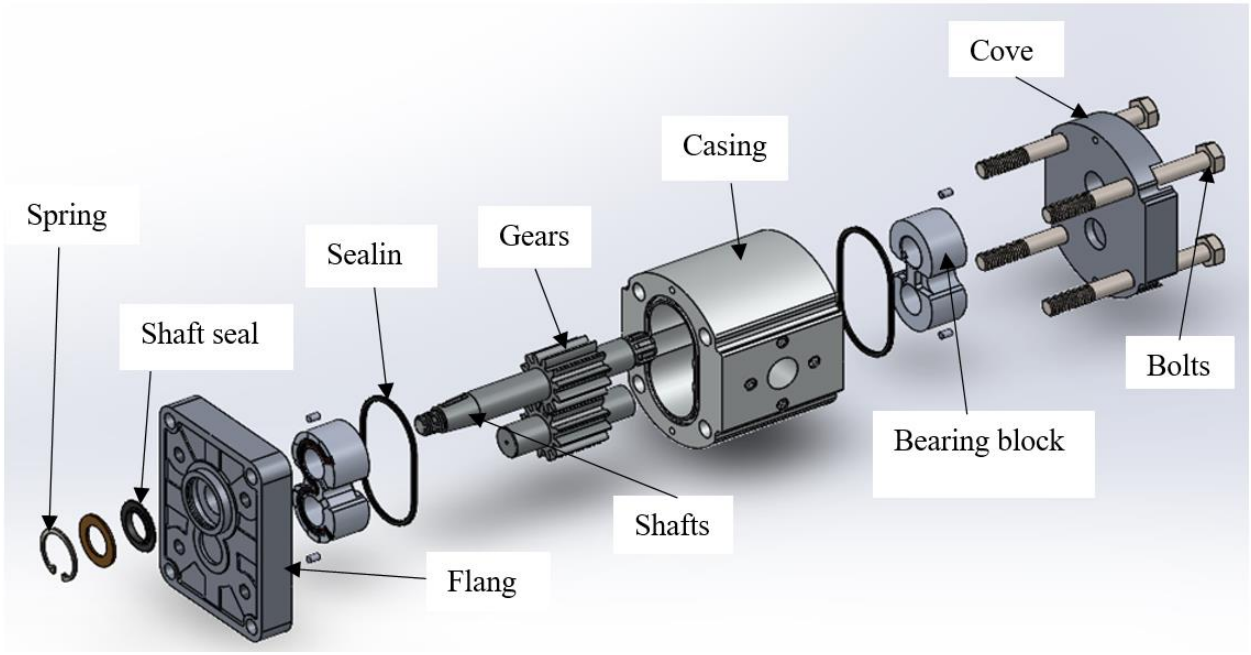

Figure 1.
Parts view of the external gear pump design.

Table 1.
Characteristics of the external gear pump.

Flow (l/min)	Max pressure (bar)	Max speed (tr/min)	Mass (g)
64.3	230	3300	3100

Table 2.
Characteristics of gears.

Number of teeth	z	12
Module [mm]	m	2.75
Circular pitch [mm]	$p = \pi \cdot m$	8.635
Pressure Angle	α	20°
Reference diameter [mm]	$d = z \cdot m$	33
Base diameter [mm]	$d_b = d \cdot \cos(\alpha)$	31.01
Tip diameter [mm]	$da = d + 2 \cdot h_a$	39.325
Root diameter [mm]	$\mathbf{d_f = d - 2.\ h_f}$	**24.84**
Face width [mm]	b	32.4
Tooth thickness on the pitch diameter [mm]	S_t	4.32
Fillet radius	$\mathbf{r_F}$	**0.96**
Tooth thickness on the tip diameter [mm]	S_a	1.06
Clearance [mm]	C	0.25
Gears entraxe[mm]	a	33

Edelweiss Applied Science and Technology
ISSN: 2576-8484
Vol. 10, No. 2: 276-296, 2026
DOI: 10.55214/2576-8484.v10i2.12036

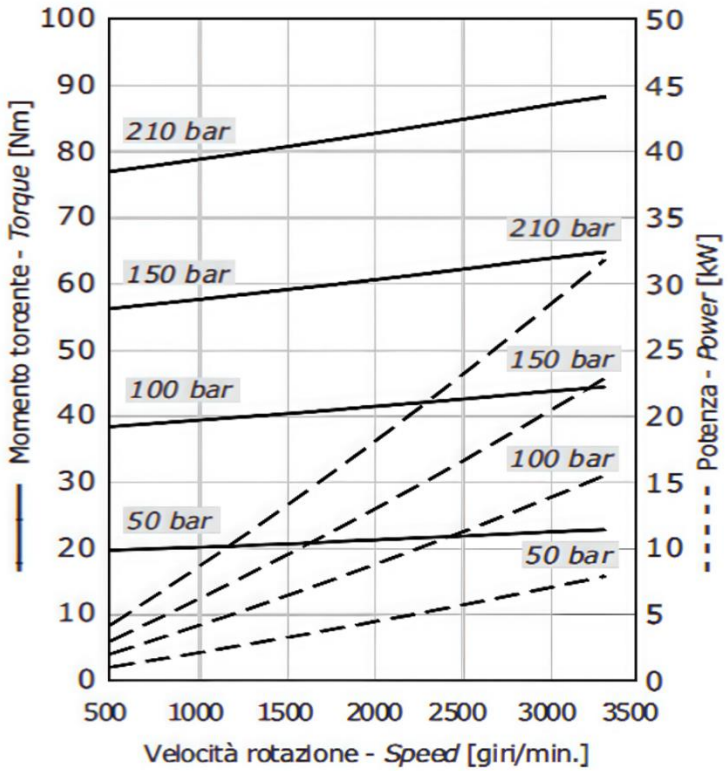

Figure 2.
Torque, speed, and power characteristics of the gear pump.

3. FEM Geometric Modeling

The gears and casing of the hydraulic gear pump were modeled in SolidWorks using the actual dimensions of the pump selected for this study, ensuring high geometric fidelity (Figures 3 and 4). To facilitate systematic resizing of the pump casing while maintaining the original geometric configuration, the SolidWorks Equation tool was utilized to link all casing dimensions to a single reference parameter (Figure 4b). This parameterized approach enables controlled and smooth reduction of the housing size without altering the fundamental design characteristics of the pump.

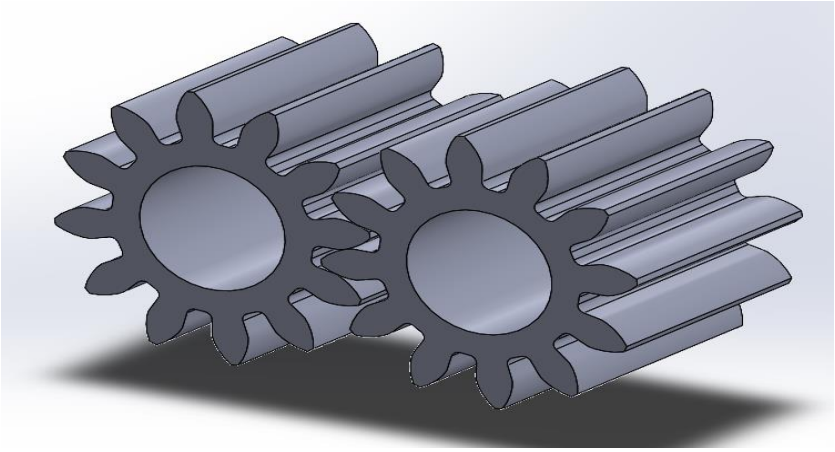

Figure 3.
Represent gears of the pump designed by SolidWorks.

Edelweiss Applied Science and Technology
ISSN: 2576-8484
Vol. 10, No. 2: 276-296, 2026
DOI: 10.55214/2576-8484.v10i2.12036

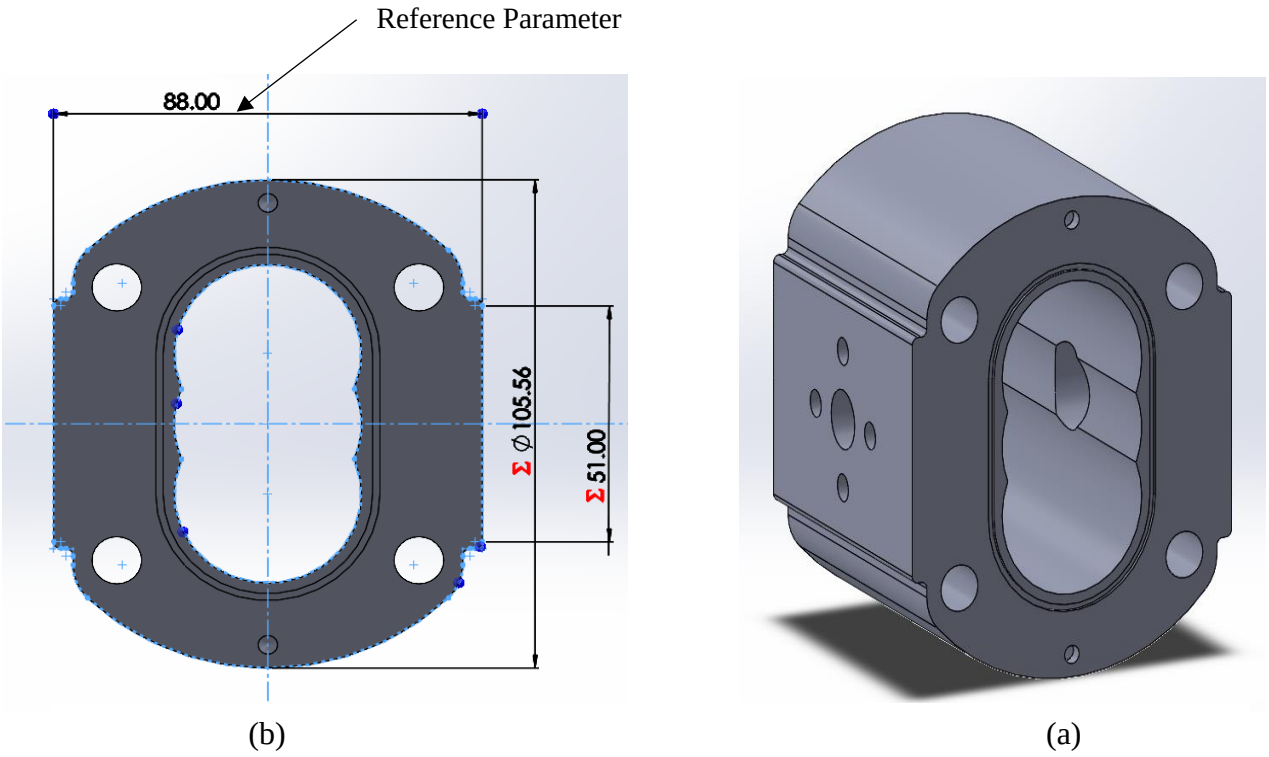

Figure 4.
Represent the gear pump casing designed by SolidWorks.

4. Finite Element Analysis

To perform this analysis, the ANSYS software package, widely recognized for its finite element analysis (FEA) capabilities, is employed, as it is particularly effective for structural and dynamic simulations. The finite element analysis is conducted in the Static Structural module of ANSYS Workbench by importing the three-dimensional model of both the gears and the pump casing from SolidWorks in SLDPRT format.

4.1. Static Structural

The Static Structural module in ANSYS is used to analyze the behavior of structures under static loading conditions, where loads are applied gradually and remain constant over time. The fundamental equation of equilibrium in mechanics governs this analysis.

$$[K]\{u\} = \{F\} \tag{1}$$

where:
$[K]$ is the stiffness matrix, representing the material and geometric properties of the structure.
$\{u\}$is the displacement vector, indicating how the structure deforms under loading.
$\{F\}$is the force vector, representing the applied external loads.

The static structural analysis aims to solve this equation to determine {u}, the deformation, and derive stresses, deformations, and reaction forces. ANSYS performs this computation using finite element methods (FEM), discretizing the structure into smaller elements for accurate results. The software also supports linear and nonlinear analyses, including geometric, material, and contact nonlinearities, making it a versatile tool for evaluating the mechanical performance of components under various conditions.

Edelweiss Applied Science and Technology
ISSN: 2576-8484
Vol. 10, No. 2: 276-296, 2026
DOI: 10.55214/2576-8484.v10i2.12036

4.2. Gears Analysis

The gears pump model is first imported, followed by mesh generation, assignment of material properties, definition of boundary conditions, and application of the appropriate operational load. Consequently, the stresses and deformation within the gears model are obtained and analyzed with the objective of optimizing its structural performance.

4.2.1. Meshing

A high-quality finite element mesh was generated for the gear models to ensure accurate resolution of stress concentrations, particularly in the fillet and root regions of the teeth. Tetrahedral elements were used with a global element size of 1 mm, which provided a suitable balance between computational efficiency and numerical accuracy. To accurately capture the contact mechanics between the mating gears, a refined mesh with an element size of 0.4 mm was applied specifically to the contact faces and along the tooth profiles. This localized refinement significantly improved the resolution of stress gradients induced by the applied torque.

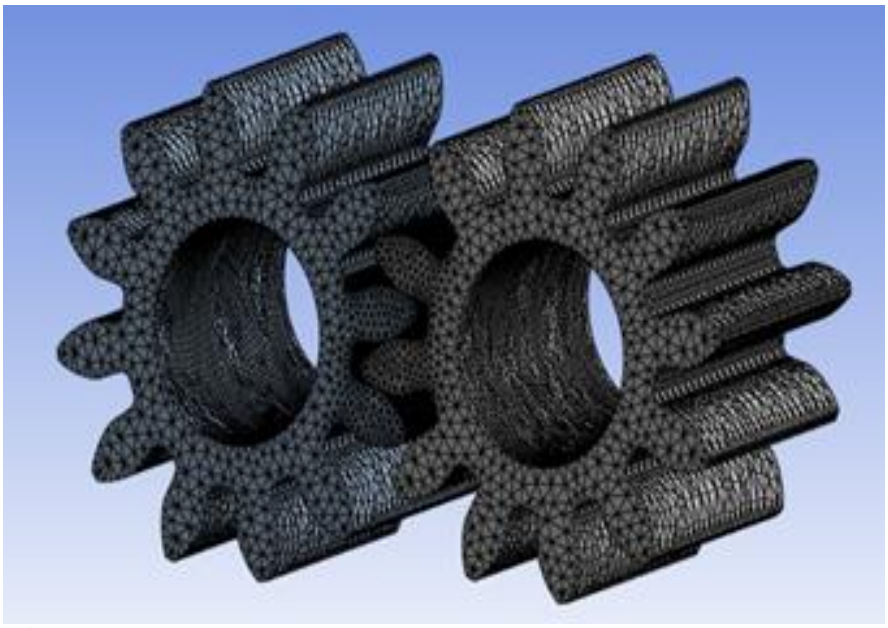

Figure 5.
Gears meshing.

4.2.2. Materiel Properties

20CrMnTi material is a case-hardening steel known for its excellent wear resistance and high surface hardness after carburizing. Its tough core and hard surface make it highly suitable for gears operating under heavy loads and repeated contact stresses.

For this reason, it is widely used in manufacturing precision gears requiring high durability and long service life.

Table 3.
20CrMnTi characteristics.

Material property	Yield strength (Mpa)	Ultimate tensile strength (Mpa)	Young's modulus (Mpa)	Density (kg/m3)	Poison ratio
20 CrMnTi	835	850	207000	7850	0.3

Edelweiss Applied Science and Technology
ISSN: 2576-8484
Vol. 10, No. 2: 276-296, 2026
DOI: 10.55214/2576-8484.v10i2.12036

4.2.3. Boundary Conditions

Figure 6 illustrates the loading and boundary conditions defined in the finite element model of the volumetric pump gears. To analyze the stresses on the gears, different boundary conditions were applied to the gear model. In the finite element analysis, the root circle of one gear is fixed, while the root circle of the second gear is constrained to allow tangential rotation but restricted in the radial direction. A torque of 88,000 N·mm is applied to the root circle of the second gear in the clockwise direction.

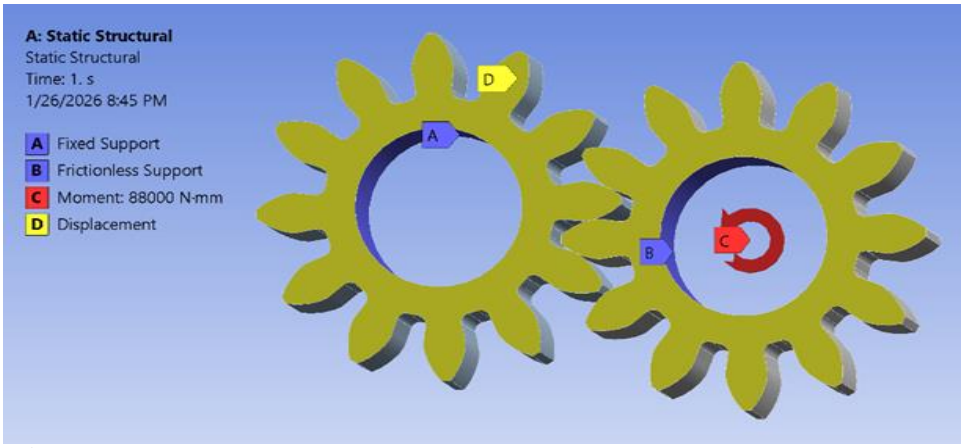

Figure 6.
Loading and boundary conditions.

4.2.4. Analysis Results and Validation

Considering the actual physics of the model generated in ANSYS, the bending stress (expressed as the equivalent von Mises stress) was evaluated. These values are presented in Figure 7.

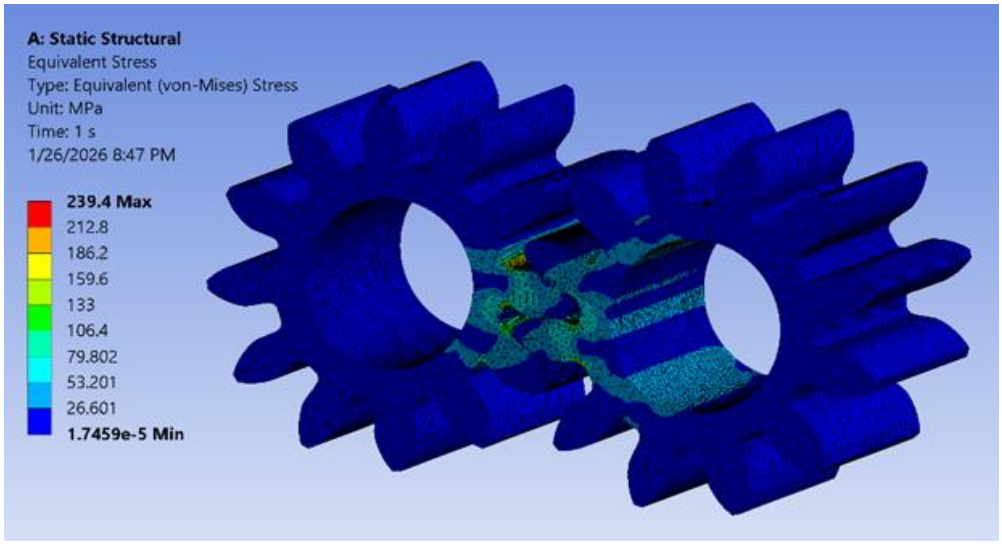

Figure 7.
Maximum Von Mises Stress ANSYS results.

To validate the accuracy of these results, the simulation results are compared with the theoretical values calculated using the Lewis method.
Lewis equation:

Edelweiss Applied Science and Technology
ISSN: 2576-8484
Vol. 10, No. 2: 276-296, 2026
DOI: 10.55214/2576-8484.v10i2.12036

$$\begin{Bmatrix} \sigma_b = \frac{6F_t h}{b{S_a}^2} \\ Y = \frac{{S_a}^2}{6hm} \\ \sigma_b = \frac{F_t}{mbY} \end{Bmatrix} \quad (2)$$

Where,
Ft: Tangential force, b: Face width of the gear, and Y: Lewis form factor, which depends on the number of teeth in the gear. In this case: Y= 0.245.
The tangential load Ft can be found from the following:

$$F_t = \frac{2T}{d_a} = \frac{2\times 88000}{33} = \frac{176000}{33} = 5333.33\ N \quad (3)$$

Then the theoretical bending stress is given by:

$$\sigma_b = \frac{5333.33}{2.75\times 32.4\times 0.245} = 244.31\ MPa \quad (4)$$

Table 4.
Comparison between Theoretical bending stress and the Von Mises stress ANSYS results.

Theoretical Bending stress (MPa)	ANSYS based Von Mises stress (MPa)	Accuracy %
244.3	239.4	97.99

From the comparison, good agreement was observed between the theoretical bending stress and the von Mises stress obtained from ANSYS. Consequently, the validity of the analysis and the results is confirmed. It is also concluded that the maximum stress generated at the tooth root remains within safe limits, considering a safety factor of 3.48.

4.3. Casing Pump Analysis

In this study, the pump casing was modeled, the mesh was generated, material properties were assigned, boundary conditions were defined, and the operational load, represented by the pump's maximum pressure, was applied. As a result, the stresses and deformations within the casing were determined.

4.3.1. Meshing

The meshing process involves dividing the entire model into small cells, with equations solved within each cell. This approach ensures result accuracy and enhances solution quality. In our case, multiple mesh configurations were applied to the same gear pump casing model developed by Kollek and Radziwanowska [31] as shown in Figure 8 and Table 4, to determine the optimal element size for our study. A moderate smoothing technique was used to generate the mesh. Additionally, second-order tetrahedral elements were employed, as they accurately represent complex geometries while maintaining a high level of precision. The patch-conforming method was applied to further improve the overall reliability and stability of the finite element analysis (FEA) model. This method simplifies the model, reduces computation time, and enhances calculation accuracy. In the current study, an element size of 1 mm was selected for the entire geometry, resulting in a total of 496,547 nodes and 293,106 elements.

Edelweiss Applied Science and Technology
ISSN: 2576-8484
Vol. 10, No. 2: 276-296, 2026
DOI: 10.55214/2576-8484.v10i2.12036

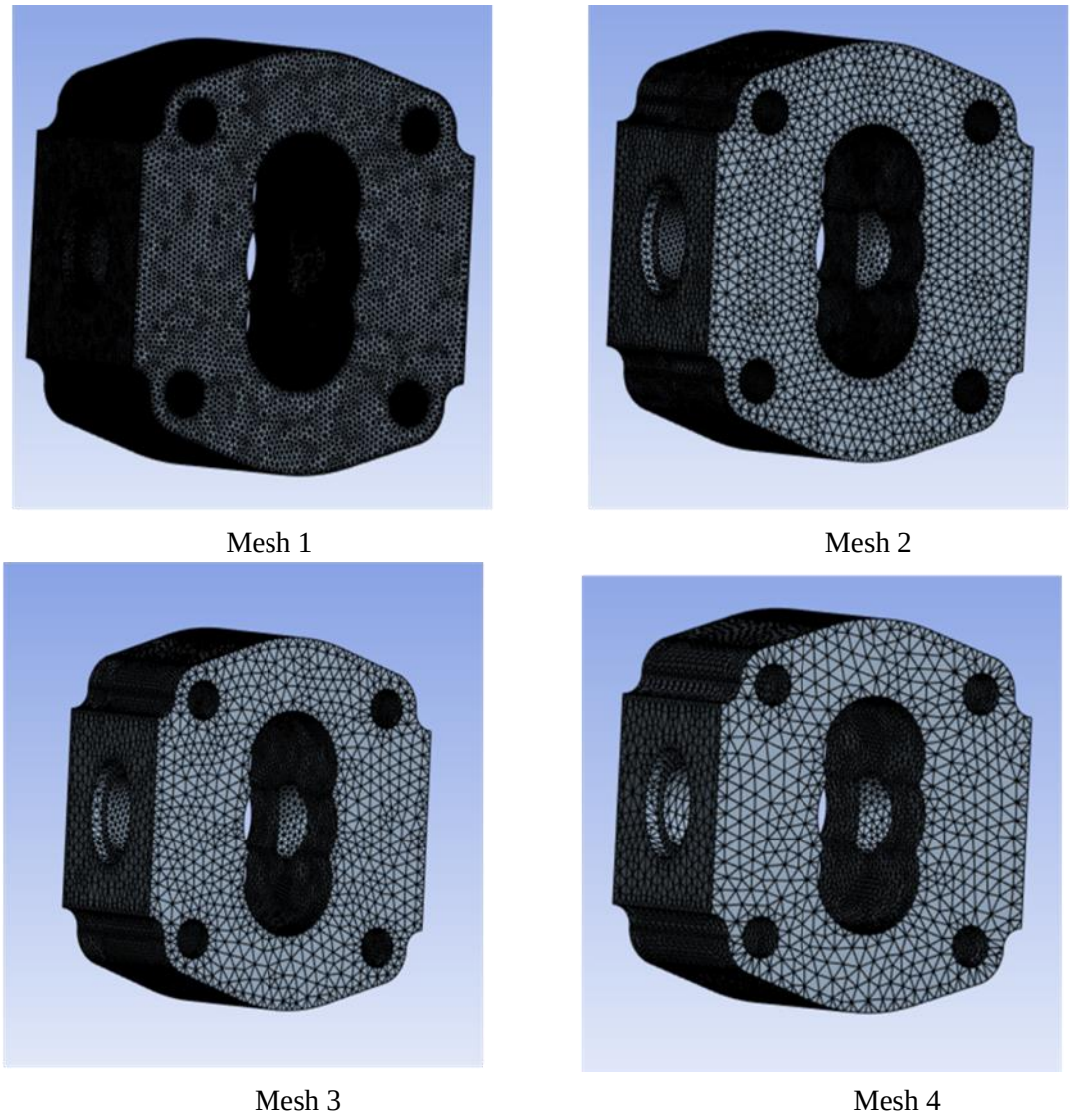

Figure 8.
Multiple meshing of gear pump casing.

Table 5.
Statistics of each mesh

Mesh type	Element size	Numbers of nodes	Numbers of elements
Mesh 1	0.4	711870	419779
Mesh 2	0.8	171785	100770
Mesh 3	1	107319	62585
Mesh 4	1.2	74273	43098

4.3.2. Materiel Properties

The gear pump casing is made of Aluminum 6061-T6 alloy, which is well known for its good strength properties, optimal balance between strength and toughness, and ease of fabrication.

Edelweiss Applied Science and Technology
ISSN: 2576-8484
Vol. 10, No. 2: 276-296, 2026
DOI: 10.55214/2576-8484.v10i2.12036

Table 6.
Presents the mechanical and physical properties of the aluminum 6061-T6 alloy.

Material property	Yield strength (Mpa)	Ultimate tensile strength (Mpa)	Young's modulus (Mpa)	Density (kg/m3)	Poison ratio
Aluminum 6061-T6 alloy	250	390	72500	2790	0.33

4.3.3. Loads and Boundary Conditions

The boundary conditions in the finite element model are based on the machine configuration. Figure 9 illustrates the loading and boundary conditions applied in the finite element model of the gear pump casing. Various boundary conditions were applied to the model to analyze the stresses on the gear pump casing. In the finite element analysis, four bolt holes are used to fix the casing components together to simulate the physical constraints of the pump during operation, ensuring no movement. Additionally, internal pressure was applied to the inner surface of the pump casing to replicate the operational pressure generated during fluid transfer, 23 MPa. This pressure load enables the software to accurately calculate the resulting stresses and deformations.

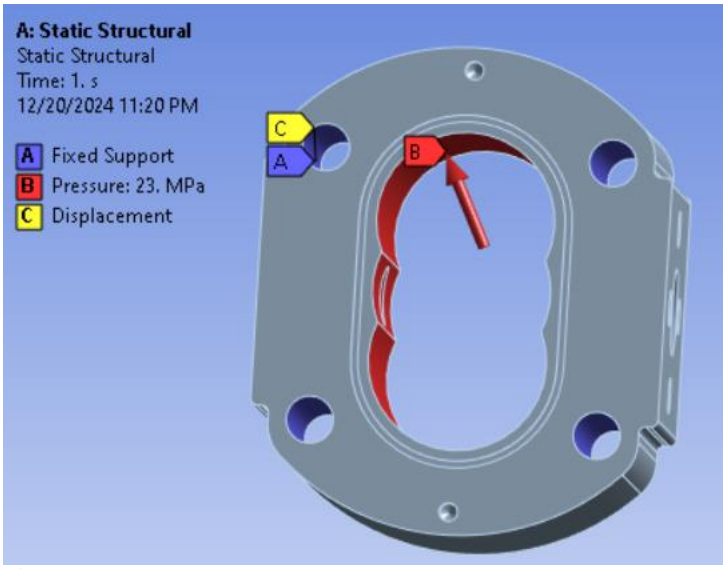

Figure 9.
Loading and boundary conditions on the gear pump casing.

4.4. Results Analysis and Validation

To validate the Finite Element Analysis (FEA) model, the stresses and deformations were compared with the study conducted by Kollek and Radziwanowska [31]. In this validation process, we used the same gear pump casing model as in their study, applying the same boundary conditions specified in their paper. This was done to determine the optimal mesh element size for our analysis. To ensure accuracy, multiple mesh configurations were applied, as previously mentioned. Table 7 presents the stress and deformation values obtained for each applied mesh. Based on these results, the mesh with an element size of 1 mm, which is the same mesh used in our study, provided the highest accuracy compared to the results from the study by Kollek and Radziwanowska [31]. Figure 10 and Table 8 offer a detailed comparison of the results, including the percentage of variation. This validation confirms the accuracy and reliability of the FEA model used in our study.

Edelweiss Applied Science and Technology
ISSN: 2576-8484
Vol. 10, No. 2: 276-296, 2026
DOI: 10.55214/2576-8484.v10i2.12036

Table 7.
Deformations and stress results for each mesh.

Mesh type	Element size of mesh (mm)	Stress (Mpa)	Deformation (mm)
Mesh 1	0.4	111.54	0.0132
Mesh 2	0.8	94.85	0.0132
Mesh 3	1	94.39	0.0132
Mesh 4	1.2	90.98	0.0132

Table 8.
Comparison of max equivalent stresses and total deformation at the gear pump casing for FEA.

	Stress	Deformation
Compared results	92.04 Mpa	0.0130 mm
Obtained results	94.39 Mpa	0.0132 mm
Variations (%)	2.55 %	1.53 %

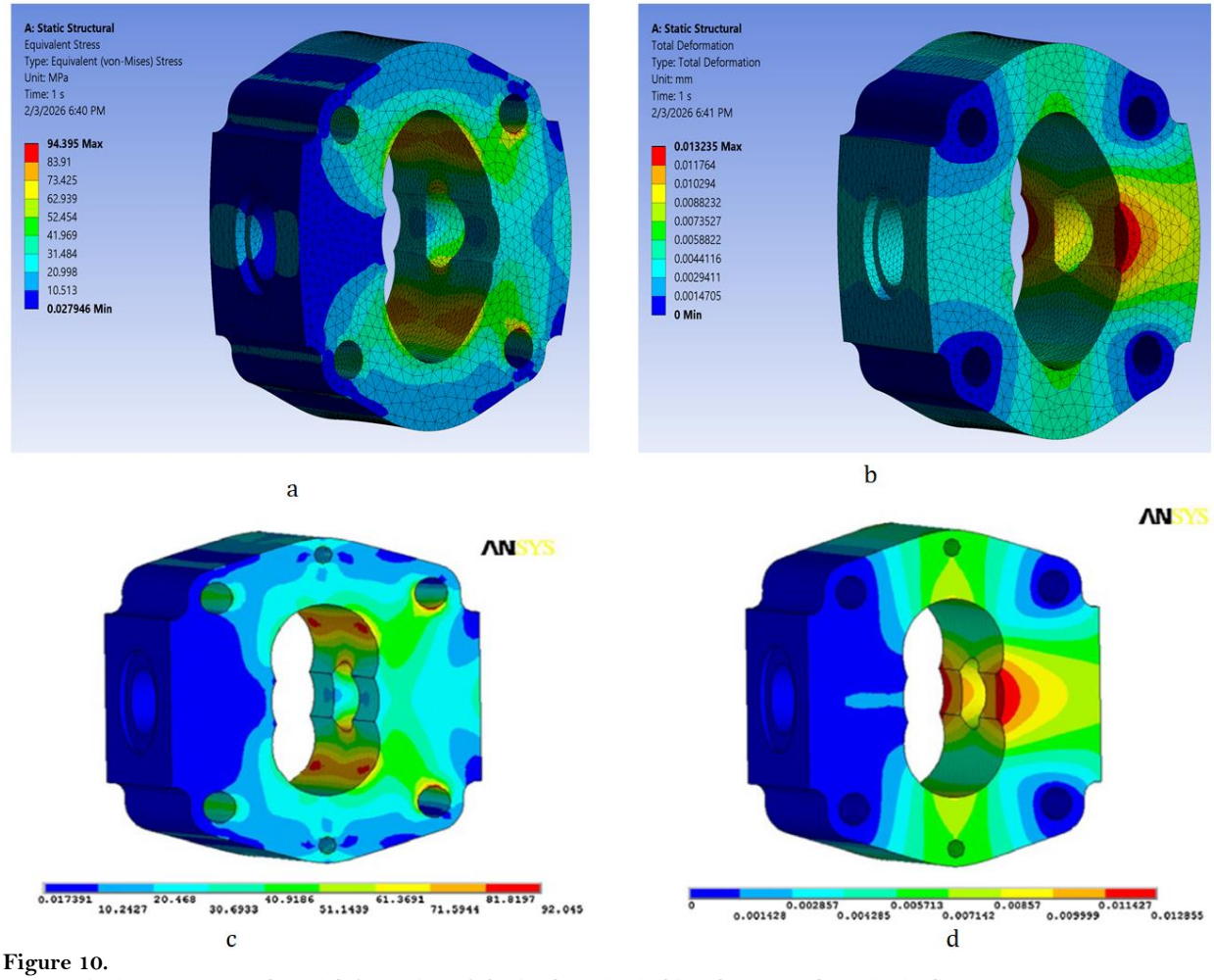

Figure 10.
Max equivalent stresses and total deformation of obtained results (a, b) and compared results (c, d).

As a result of the simulation, the stress and deformation distributions in the gear pump casing were obtained, Figures 11 (a, b). From Figure 11(a), it is clear that the most loaded part of the gear pump casing is the liner block area on the inner side of the pump casing on the discharge side, where the maximum value reached 98 MPa. The areas around the bolt holes on the right side of the pump casing and the outer

Edelweiss Applied Science and Technology
ISSN: 2576-8484
Vol. 10, No. 2: 276-296, 2026
DOI: 10.55214/2576-8484.v10i2.12036

edge of the discharge channel are subjected to high stress levels. However, the maximum stress remains much lower than the tensile strength (390 MPa) of the aluminum 6061-T6 alloy. In this case, Figure 11(c) shows that the safety factor is 3.9, which ensures reliable structural performance. The stress values become smaller than the maximum value in the rest of the casing. On the suction side, the stress values are very small. The total deformation value, as shown in Figure 11(b), is approximately 0.024 mm. The highest recorded total deformation occurs on the inner side of the gear pump casing, specifically in the discharge channel area.

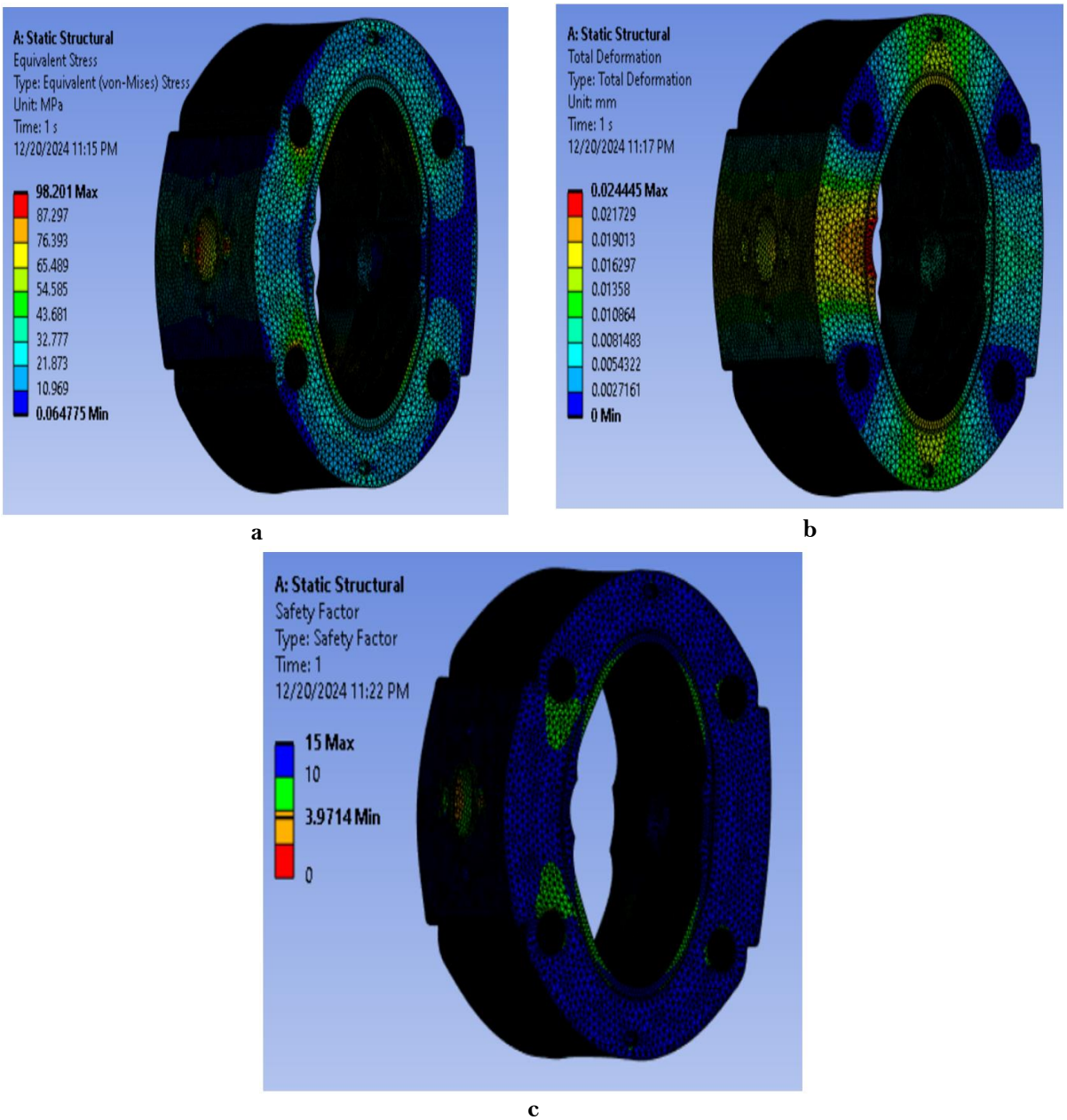

Figure 11.
Equivalent Stress and total deformation with a safety factor generated on the gear pump casing.

Edelweiss Applied Science and Technology
ISSN: 2576-8484
Vol. 10, No. 2: 276-296, 2026
DOI: 10.55214/2576-8484.v10i2.12036

Based on the simulation results obtained for the external gear pump casing model, the stress and deformation values are significantly lower than the allowable limit. In light of this finding, it was decided to optimize the external gear pump casing by reducing its mass to achieve our objective of minimizing the material used in its manufacturing while ensuring a high energy efficiency ratio for the pump, all while maintaining its overall performance.

To accomplish this, the pumping unit, bearings, and the dimensions of the suction and discharge ports were kept unchanged. The optimization criterion focused on minimizing the pump casing mass to the lowest possible level while ensuring an optimal distribution of stresses and deformations. The goal was to reduce the casing dimensions as much as possible while ensuring that stress and deformation values remained within acceptable engineering limits.

5. Results and Discussion

In the optimization of the gear pump casing, mathematical tools and predefined constraints are employed to determine the most efficient design [29]. Various optimization techniques can be utilized, including Response Surface Methodology (RSM) [16] and the Taguchi method [32]. RSM is widely used to optimize outcomes influenced by multiple input variables. In this study, we adopted RSM to achieve our objective.

In the first stage of optimization, the focus was on improving the geometry of the pump gears to enhance their load-carrying capacity. In this shape optimization approach, not all gear dimensions are modified; only selected design variables are adjusted within allowable limits to avoid compromising the volumetric efficiency of the pump.

In this methodology, the design variables include the fillet radius and the root radius of the gear, as summarized in Table 9.

Table 9.
The design parameters variables.

Design variables	Lower bound	Upper bound
fillet radius (mm)	0.84	1.82
Root radius (mm)	12.2	12.4

The finite element analysis, carried out within the Response Surface Methodology (RSM) framework, examines the effects of varying the gear fillet radius at the tooth root and the tooth height to obtain the von Mises stresses generated at the critical location under loading. The influence of these design parameters on the von Mises stress at the critical zones was evaluated while ensuring that the pump's volumetric efficiency remained unaffected. Table 10 presents the stress values resulting from variations in the gear's fillet radius and root radius.

Table 10.
The max equivalent stress response results of DEO.

Root Fillet	Root Radius	Equivalent Stress Maximum (MPa)
1.27	12.3	224.79
0.93	12.3	262.33
1.82	12.2	211.75
1.53	12.4	217.44
0.84	12.4	271.01

Based on the results of the load and stress analysis, geometric improvements were achieved for the pump gear design. Table 11 presents a comparison of the von Mises stresses between the optimized gears and the original configuration. Owing to these improvements, the stresses were reduced from 239.4 MPa to 224.79 MPa. Consequently, the geometric optimization resulted in a 6.1% reduction in von Mises stress at the critical region compared with the original gear design. This reduction is attributed to localized geometric modifications, specifically increasing the fillet radius from 0.93 mm to 1.27 mm, followed by

Edelweiss Applied Science and Technology
ISSN: 2576-8484
Vol. 10, No. 2: 276-296, 2026
DOI: 10.55214/2576-8484.v10i2.12036

adjusting the root radius from 12.43 mm to 12.3 mm. These changes effectively decrease the von Mises stresses generated in the gears.

Table 11.
Comparison of the von Mises stresses between the optimized gears and the original gears.

Optimized gears	**Original gears**	
von Mises stress (MPa)	von Mises stress (MPa)	Reduction (%)
224.79	239.40	6.10

To achieve our objective of reducing stresses at the gear tooth roots, thereby extending the pump's service life and improving its performance while maintaining volumetric efficiency, the optimal gear design was identified. Table 12 presents the optimal configuration for the pump gears, derived from the Design of Experiments (DOE) table. This design represents a balanced solution that enhances structural efficiency in terms of strength and durability, ensuring mechanical reliability under the specified loading conditions.

Table 12.
Presents the optimal gear design.

	Filte radius (mm)	**Root radius (mm)**	**von Mises stress (MPa)**
Optimal design	1.27	12.3	224.79

Secondly, to achieve the desired objective of obtaining an optimized design that reduces mass and conserves materials while ensuring a high efficiency ratio, we first defined the geometric dimensions in the optimization methodology. These include the reference dimension of the pump casing and the diameter of the bolt holes, as shown in Table 13.

The pump casing mass, maximum total deformation, and maximum equivalent stress are set as output parameters.

Using the Central Composite Design (CCD) method with a single central point for Design of Experiments (DOE) [33], 9 results were obtained in ANSYS. The results are presented in Table 7.

Table 13.
Variables valus of input design parameters.

Design variables	**Lower bound**	**Upper bound**
Reference parameter (mm)	74	84
Bolt holes diameter (mm)	8.2	11

Table 14.
The mass, total deformation, and the max equivalent stress response results of DEO.

Design point	**Reference parameter (mm)**	**Bolt holes diameter (mm)**	**Total deformation (mm)**	**Max equevalent stress (Mpa)**	**Mass (kg)**
01	79	9.6	0.033	131.79	0.814
02	74	9.6	0.040	160.89	0.666
03	84	9.6	0.027	112.46	0.973
04	79	8.2	0.034	135.88	0.831
05	79	11	0.031	127.85	0.795
06	74	8.2	0.042	170.62	0.683
07	84	8.2	0.029	120.55	0.990
08	74	11	0.038	152.34	0.647
09	84	11	0.026	106.82	0.953

To optimize the design of the external gear pump casing, a comprehensive sensitivity analysis is useful for assessing the significance of design parameters. This analysis is conducted while all input variables change simultaneously, and sensitivity is evaluated across the full range of each design parameter.

Edelweiss Applied Science and Technology
ISSN: 2576-8484
Vol. 10, No. 2: 276-296, 2026
DOI: 10.55214/2576-8484.v10i2.12036

It is important to note that a positive sensitivity of the output response to an input parameter indicates that as the design parameter increases, the output parameter also increases. Conversely, a negative sensitivity means that an increase in the design parameter leads to a decrease in the output parameter.

Figure 12 presents the results of the sensitivity analysis. The findings indicate that the reference parameter has a significant impact on all output responses. Specifically, both equivalent stress and total deformation exhibit an inverse relationship with the sensitivity value of the reference parameter. A decrease in the reference parameter leads to an increase in both equivalent stress and total deformation.

Furthermore, the pump casing mass shows a positive correlation with the sensitivity value of the reference parameter. This means that a reduction in the reference parameter results in a decrease in the pump casing mass.

On the other hand, all output responses, equivalent stress, total deformation, and pump casing mass, demonstrate an inverse relationship with the sensitivity value of the clearance hole diameter for bolts. In other words, as the clearance hole diameter increases, all output values decrease.

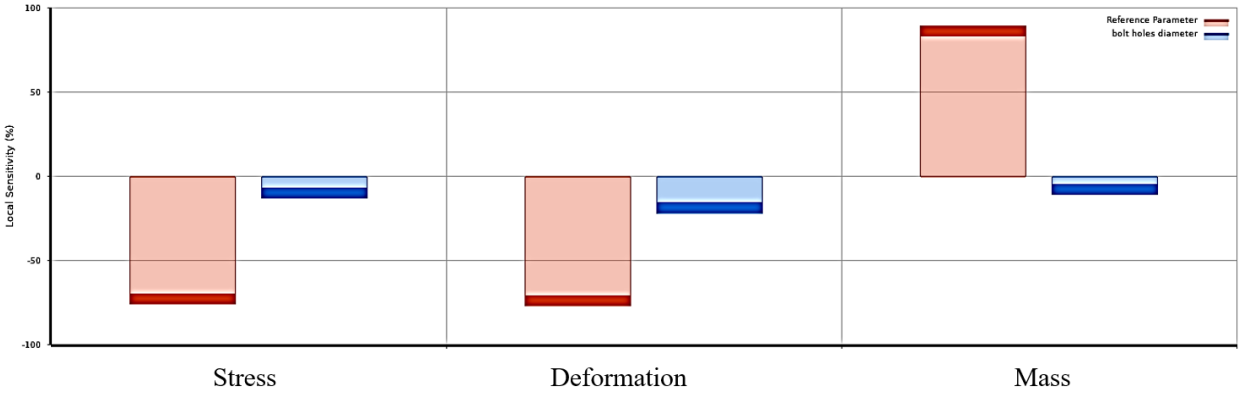

Figure 12.
Results of the sensitivity analysis.

The input parameters were selected based on the most sensitive factors for each output. The response surface was generated using the results of the design of experiments (DOE) for deformation, stress, and mass. Figure 13 (a, b) illustrates that as the clearance hole diameter for bolts increases, both equivalent stress and total deformation gradually decrease.

However, a reduction in the reference parameter results in a significant increase in both equivalent stress and total deformation, highlighting the strong influence of the reference parameter on these outputs.

Edelweiss Applied Science and Technology
ISSN: 2576-8484
Vol. 10, No. 2: 276-296, 2026
DOI: 10.55214/2576-8484.v10i2.12036

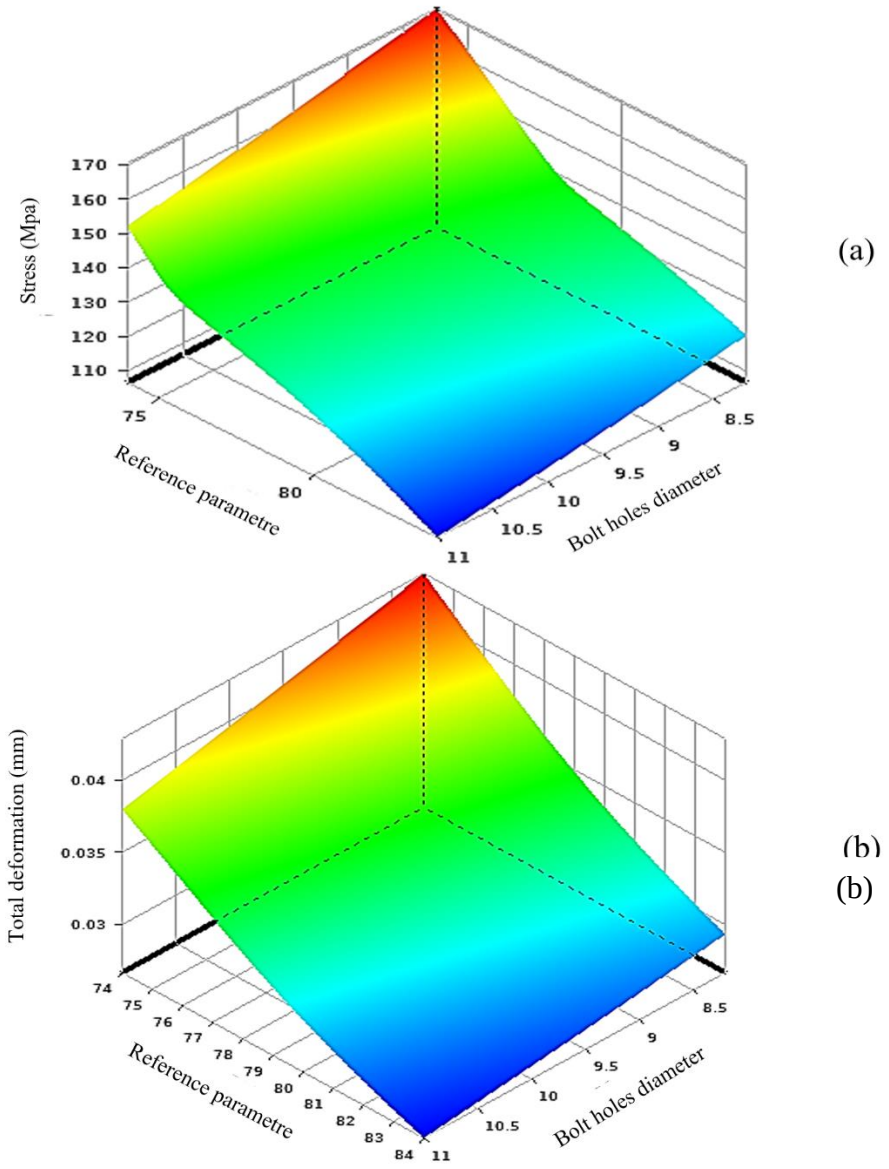

Figure 13.
Response surface of the input parameters on equivalent stress and total deformation.

Additionally, Figure 14 shows that an increase in the clearance hole diameter leads to a slight and gradual reduction in the pump casing mass. In contrast, a noticeable decrease in the pump casing mass is observed when the reference parameter is reduced, further emphasizing its significant impact on the pump casing mass.

Edelweiss Applied Science and Technology
ISSN: 2576-8484
Vol. 10, No. 2: 276-296, 2026
DOI: 10.55214/2576-8484.v10i2.12036

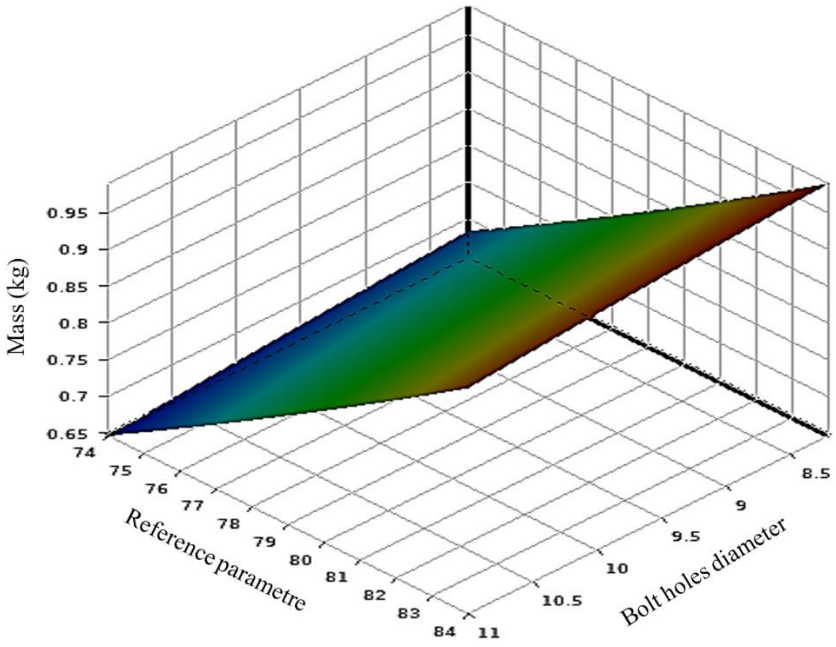

Figure 14.
Response surface of the input parameters on the gear pump casing.

To achieve our objective of reducing the pump casing mass while maintaining the safety factor within the acceptable limit

$$S_f = \frac{\sigma_n}{\sigma} = \frac{390}{127.85} = 3.05 \quad (5)$$

Table 15 presents the optimized design of the gear pump casing, derived from the design of experiments (DOE) table. This design strikes a balance between structural efficiency and material economy, ensuring that the casing remains both lightweight and mechanically reliable under the specified loading conditions.

Table 15.
The optimal design of the gear pump casing.

	Reference parameter (mm)	Bolt holes diameter (mm)	Mass (kg)
Optimal design	79	11	0.795

The efficiency to mass ratio of a gear pump is a metric used to evaluate its efficiency by comparing the energy it produces to its mass. This ratio is calculated by dividing the pump's output power by its mass [31].

$$K_{e_f} = \frac{P}{m} \quad (6)$$

where:
K_{e_f}: The efficiency to mass ratio of a gear pump P: The power produced by the pump, measured in Watts (W).

$$P = Q(m^3/s) \times p \quad \text{(Pa)} \quad (7)$$

$$P = 1.07 \times 10^{-3}(m^3/s) \times 23 \times 10^6 \quad \text{(Pa)} \quad \rightarrow \quad P = 24610 \quad \text{(Watt)} \quad (8)$$

m : The mass of the pump, measured in grams (g).

The efficiency-to-mass ratio is a key indicator of design effectiveness. The higher the ratio, the more efficient the pump is in generating energy relative to its weight, making it ideal for applications requiring

Edelweiss Applied Science and Technology
ISSN: 2576-8484
Vol. 10, No. 2: 276-296, 2026
DOI: 10.55214/2576-8484.v10i2.12036

lightweight and energy-efficient operation. Additionally, pumps with a high ratio help reduce operating costs and extend their service life, making them a cost-effective and efficient choice in the long run.

Before calculating the efficiency to mass ratio, the total mass of both the original and optimized pumps is determined. Notably, the dimensions of the flange and rear cover have been reduced to align with the optimized design of the gear pump casing. Table 16 presents the total mass values for both the original and optimized pumps.

Table 16.
Total mass values of the original pump and optimized pump.

Gear pumps	Original pump (g)	Optimized pump (g)	Percentage optimized (%)
Total mass (kg)	3100	2805	9.5%

Based on the mass values listed in Table 16 for both pumps and considering the previously calculated power of the external gear pump, the efficiency-to-mass ratio for both pumps was calculated.

a) Original gear pump:

$$K_{e_f} = \frac{24610}{3100} = 7.9 \tag{9}$$

b) Optimized gear pump:

$$K_{e_f} = \frac{24610}{2805} = 8.8 \tag{10}$$

Table 17.
Efficiency to mass ratio values of both pumps with percentage optimized

Parameters	Original pump	Optimized pump
Efficiency to mass ratio (w/g)	7.9	8.8
Percentage optimized (%)	11.4	

Based on this calculation and the values presented in Table 17, it is evident that the efficiency-to-mass ratio of the optimized pump is 8.8, which is significantly higher than that of the original design, which was 7.9. This represents an 11.4% improvement compared to the original design.

This enhancement is primarily due to a 9.5% weight reduction in the pump casing while maintaining the key components unchanged, including the pumping unit size, which consists of the driving and driven gears, as well as the bushings and the inlet and outlet port diameters. Additionally, the overall efficiency of the pump was preserved without any negative impact, ensuring an optimal balance between weight reduction and operational performance improvement. The optimized gear pump design, with its increased power-to-mass ratio, contributes to lower operating costs and an extended service life, making it a cost-effective and efficient choice in the long run, particularly for applications requiring lightweight and high-efficiency operation.

6. Conclusion

In this paper, a comprehensive finite element analysis was performed on both the casing and gear components of an external gear pump to enhance structural performance and reduce material consumption. For the pump casing, structural simulations in ANSYS revealed that the maximum stress and deformation in the original design were 98 MPa and 0.024 mm, respectively, corresponding to a safety factor of 3.9. Using the Response Surface Methodology (RSM), the reference parameter and bolt hole diameter were selected as design variables, and nine design points were evaluated. The optimal configuration, 79 mm for the reference parameter and 11 mm for the bolt hole diameter, exhibited a stress of 127 MPa, a deformation of 0.031 mm, and a safety factor of 3. This optimization yielded a notable reduction in casing mass from 3.1 kg to 2.79 kg, representing over 9.5% weight savings, while also improving the energy efficiency ratio from 7.9 to 8.8. Parallel optimization of the pump gears led to additional structural enhancements. By modifying key geometric features, specifically increasing the fillet

Edelweiss Applied Science and Technology
ISSN: 2576-8484
Vol. 10, No. 2: 276-296, 2026
DOI: 10.55214/2576-8484.v10i2.12036

radius from 0.93 mm to 1.27 mm and adjusting the root radius from 12.43 mm to 12.3 mm, the von Mises stress was reduced from 239.4 MPa to 224.79 MPa, a 6.1% decrease in the critical region. These improvements confirm that targeted geometric refinement, supported by finite element simulations and RSM-based optimization, can significantly enhance structural integrity, reduce mechanical stresses, and improve the overall performance and efficiency of hydraulic gear pumps.

Transparency:

The authors confirm that the manuscript is an honest, accurate, and transparent account of the study; that no vital features of the study have been omitted; and that any discrepancies from the study as planned have been explained. This study followed all ethical practices during writing.

Copyright:

References

[1] H.-y. Yang and M. Pan, "Engineering research in fluid power: A review," *Journal of Zhejiang University-Science A*, vol. 16, no. 6, pp. 427-442, 2015. https://doi.org/10.1631/jzus.A1500042

[2] C. Ferrari, S. Morselli, G. Miccoli, and K. Hamiche, "Integrated CFD-FEM approach for external gear pump vibroacoustic field prediction," *Frontiers in Mechanical Engineering*, vol. 10, p. 1298260, 2024. https://doi.org/10.3389/fmech.2024.1298260

[3] M. Borghi, B. Zardin, and E. Specchia, *External gear pump volumetric efficiency: Numerical and experimental analysis (SAE Technical Paper 2009-01-2844)*. Warrendale, PA, USA: SAE International, 2009.

[4] A. Vacca and M. Guidetti, "Modelling and experimental validation of external spur gear machines for fluid power applications," *Simulation Modelling Practice and Theory*, vol. 19, no. 9, pp. 2007-2031, 2011. https://doi.org/10.1016/j.simpat.2011.05.009

[5] I. Ghionea, A. Ghionea, and G. Constantin, "CAD-CAE methodology applied to analysis of a gear pump," *Proceedings in Manufacturing Systems*, vol. 8, no. 1, pp. 1-6, 2013.

[6] P. Casoli, A. Vacca, and B. GL, "Optimization of relevant design parameters of external gear pumps," in *Proceedings of the JFPS International Symposium on Fluid Power (Vol. 2008, No. 7-2, pp. 277-282). The Japan Fluid Power System Society*, 2008.

[7] P. Casoli, A. Vacca, and G. Franzoni, "A numerical model for the simulation of external gear pumps," in *In Proceedings of the JFPS International Symposium on Fluid Power (Vol. 2005, No. 6, pp. 705-710). The Japan Fluid Power System Society*, 2005.

[8] H. Li, C. Yang, and P. Zhou, "The finite element analysis and optimizations of shells of internal gear pumps based on ansys," in *Proceedings of 2011 International Conference on Fluid Power and Mechatronics (pp. 185-190). IEEE*, 2011.

[9] A. P. Agrawal, S. Ali, and S. Rathore, "Finite element stress analysis for shape optimization of spur gear using ANSYS," *Materials Today: Proceedings*, vol. 64, pp. 1147-1152, 2022. https://doi.org/10.1016/j.matpr.2022.03.404

[10] B. Zheng and J. Zhang, "Contact stress and modal analysis of gear pump," presented at the 12th International Conference on Intelligent Computation Technology and Automation (ICICTA) (pp. 654-657). IEEE, 2019.

[11] M. Bulut and Ö. Cihan, "Stress and deformation analysis of a connecting rod by using ANSYS," *International Journal of Automotive Engineering and Technologies*, vol. 9, no. 3, pp. 154-160, 2020. https://doi.org/10.18245/ijaet.680511

[12] S. Taskaya and S. Taskaya, "Investigation of static structure effect according to axial coordinates by using finite element method in Ansys workbench software of AISI 310 austenitic stainless cylindrical model steel," *International Journal of Scientific Engineering and Science*, vol. 2, no. 11, pp. 65-70, 2018.

[13] F. Guo and H. Du, "Modal analysis of components and whole of gear pump," in *IOP Conference Series: Earth and Environmental Science (Vol. 632, No. 3, p. 032005). IOP Publishing*, 2021.

[14] L. Cheng, H.-B. Lin, and Y.-L. Zhang, "Optimization design and analysis of mobile pump truck frame using response surface methodology," *PLoS One*, vol. 18, no. 8, p. e0290348, 2023. https://doi.org/10.1371/journal.pone.0290348

[15] A. Trad, N. Amoura, A. Abdellah Elhadj, and H. Kebir, "Optimizing plastic shredder rotor design through structural finite element analysis: A comprehensive approach using experimental design and response surface methodology," *Mechanics Based Design of Structures and Machines*, vol. 52, no. 12, pp. 10682-10701, 2024. https://doi.org/10.1080/15397734.2024.2360680

[16] N. Mansouri, M. Moghimi, and M. Taherinejad, "Investigation on hydrodynamics and mass transfer in a feed channel of a spiral-wound membrane element using response surface methodology," *Chemical Engineering Research and Design*, vol. 149, pp. 147-157, 2019. https://doi.org/10.1016/j.cherd.2019.07.006

Edelweiss Applied Science and Technology
ISSN: 2576-8484
Vol. 10, No. 2: 276-296, 2026
DOI: 10.55214/2576-8484.v10i2.12036

[17] A. A. El-Hadj and S. Z. B. Abd Rahim, "Optimization of an external gear pump using response surface method," *Journal of Mechanics*, vol. 36, no. 4, pp. 567-575, 2020. https://doi.org/10.1017/jmech.2020.7

[18] Y. Yoon, B.-H. Park, J. Shim, Y.-O. Han, B.-J. Hong, and S.-H. Yun, "Numerical simulation of three-dimensional external gear pump using immersed solid method," *Applied Thermal Engineering*, vol. 118, pp. 539-550, 2017. https://doi.org/10.1016/j.applthermaleng.2017.03.014

[19] V. Ivanov, D. Karaivanov, S. Ivanova, and M. Volkova, "Gear mesh geometry effect on performance improvement for external gear pumps," in *MATEC Web of Conferences (Vol. 287, p. 01007). EDP Sciences*, 2019.

[20] K. Kattimani, R. Tavildar, and P. Kakamari, "Finite element analysis and optimization of external gear pump," *Jetir*, vol. 3, pp. 119-126, 2016.

[21] S. Gulati, A. Vacca, and M. Rigosi, "A general method to determine the optimal profile of porting grooves in positive displacement machines: the case of external gear machines," 2016.

[22] R. Cieślicki and M. Karpenko, "An investigation of the impact of pump deformations on circumferential gap height as a factor influencing volumetric efficiency of external gear pumps," *Transport*, vol. 37, no. 6, pp. 373-382, 2022.

[23] W. Kollek, P. Osiński, and U. Warzyńska, "The influence of gear micropump body asymmetry on stress distribution," *Polish Maritime Research*, vol. 24, no. 1 (93), pp. 60-65, 2017.

[24] R. Cieślicki, J. Karliński, and P. Osiński, "Numerical model of an external gear pump and its validation," in *International Conference on Computer Aided Engineering (pp. 96-103). Cham: Springer International Publishing*, 2018.

[25] F. Guo, "Finite element analysis and optimization of CBY-100 gear pump body," in *Journal of Physics: Conference Series (Vol. 1622, No. 1, p. 012116). IOP Publishing*, 2020.

[26] I. G. Ghionea, "Applied methodology for designing and calculating a family of spur gear pumps," *Energies*, vol. 15, no. 12, p. 4266, 2022. https://doi.org/10.3390/en15124266

[27] L. Rodionov *et al.*, "Challenges in design process of gear micropump from plastics," *Archives of Civil and Mechanical Engineering*, vol. 21, p. 34, 2021. https://doi.org/10.1007/s43452-020-00164-5

[28] O. Zharkevich *et al.*, "Parametric optimization of a new gear pump casing based on weight using a finite element method," *Applied Sciences*, vol. 13, no. 22, p. 12154, 2023. https://doi.org/10.3390/app132212154

[29] M. Ozsoy and C. Kurnaz, "An optimization study of a hydraulic gear pump cover with finite element method," *Acta Physica Polonica A*, vol. 132, no. 3, pp. 944-948, 2017.

[30] W. Kollek and U. Radziwanowska, "The modernization of gear micropump casing with the use of finite element method," *IMPACT: International Journal of Research in Engineering & Technology (IMPACT: IJRET)*, vol. 2, no. 7, pp. 69-76, 2014.

[31] W. Kollek and U. Radziwanowska, "Energetic efficiency of gear micropumps," *Archives of Civil and Mechanical Engineering*, vol. 15, no. 1, pp. 109-115, 2015. https://doi.org/10.1016/j.acme.2014.05.005

[32] M. Yanikören, "Experimental investigation of the performance and energy consumption efficiency of elliptical gear hydraulic pump and evaluation by Taguchi method," *Engineering Science and Technology, an International Journal*, vol. 62, p. 101941, 2025. https://doi.org/10.1016/j.jestch.2024.101941

[33] A. S. Okouzi, A. O. A. Ibhadode, and A. I. Obanor, "Response surface methodology (RSM) optimization of the batch process in a rectangular passive greenhouse dryer," *International Journal of Engineering Research in Africa*, vol. 56, pp. 145-161, 2021.